Materials & Design 126 (2017) 197–206

Contents lists available at ScienceDirect

Materials & Design

journal homepage: www.elsevier.com/locate/matdes

Laser-induced exothermic bonding of carbon fiber/Al composites and TiAl alloys

Guangjie Feng[a,b], Zhuoran Li[a,*], Rohit J. Jacob[b,c], Yong Yang[b], Yu Wang[a], Zhi Zhou[a], Dusan P. Sekulic[a,d], Michael R. Zachariah[b,c]

[a] State Key Laboratory of Advanced Welding and Joining, Harbin Institute of Technology, Harbin 150001, China
[b] Department of Chemical and Biomolecular Engineering, University of Maryland, College Park, MD 20742, USA
[c] Department of Chemistry and Biochemistry, University of Maryland, College Park, MD 20742, USA
[d] Department of Mechanical Engineering, College of Engineering, University of Kentucky, Lexington, KY 40506, USA

ARTICLE INFO

Keywords:
Laser-induced exothermic reaction
C_f/Al composites
TiAl alloys
Microstructure
Mechanical property
Welding

ABSTRACT

In this paper, a highly-efficient method for bonding Carbon Fiber (C_f)/Al composites and TiAl alloys was developed by means of laser-induced exothermic reaction of a Ni-Al-Ti interlayer. To examine the interlayer exothermic performance, the adiabatic temperature was calculated and the reaction temperatures were measured. Based on SEM, XRD and TEM, the interfacial reactions between carbon fiber and interlayer products were investigated. Results show that the addition of Ti enhanced the interfacial reactions between carbon fibers and interlayer products. The resulting formation of a 300–400 nm thin Ti-C layer at the $NiAl_3$/carbon fiber interface was identified as a key player in improving the joining quality on the C_f/Al side. The typical interfacial structure of the joint is (C_f/Al)/Ti-C/$NiAl_3$/Ni_2Al_3/(NiAl + Al_3NiTi_2)/Al_3NiTi_2/TiAl. The joint formation mechanism was discussed. In addition, the effect of Ti content on the microstructure and mechanical properties of joints were investigated in detail. The optimum value of Ti content was found to be 5 wt.%, leading to a defect-free joint and a maximum shear strength of 45.8 MPa.

GRAPHICAL ABSTRACT

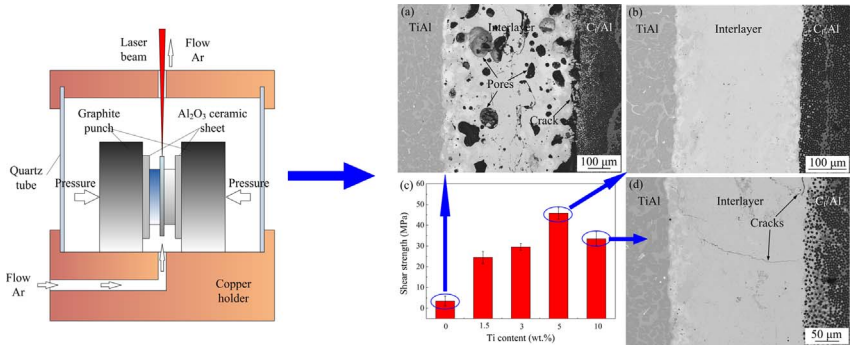

1. Introduction

Carbon Fibers possessing high Young's modulus, superior tensile strength, low density, as well as excellent electrical and thermal conductivities [1–3], are considered as ideal reinforcements for metal matrix composites (MMCs). Owing to their attractive mechanical, thermal and physical properties [4], Carbon Fiber reinforced aluminum matrix composites (C_f/Al) are expected to replace traditional materials,

* Corresponding author.
E-mail address: lizr@hit.edu.cn (Z. Li).

http://dx.doi.org/10.1016/j.matdes.2017.04.044
Received 10 March 2017; Received in revised form 10 April 2017; Accepted 12 April 2017
Available online 13 April 2017

and have been implemented for several successful applications in waveguide tubes and antenna frames on satellites as well in more structurally challenging applications like the aircraft body [5,6]. TiAl alloys (featuring light weight, high melting point and good oxidation resistance [7,8]) are also promising materials in automobile and aerospace fields [9]. Successful joining C_f/Al composites to TiAl alloys can produce composite structures with combined advantages, with the potential for new applications [10].

Unfortunately, such a joining is a significant challenge due to the inevitably large differences in the chemical and physical properties between C_f/Al composites and TiAl alloys. Brazing, which is a widely-used technique to join dissimilar materials [11], is not suitable for the C_f/Al-TiAl joining couple because of the difficulty in finding ideal filler metals. This is mainly caused by the significant difference in melting points (about 1733 K for TiAl alloys versus about 930 K for Al in the C_f/Al matrix). The common filler metals for TiAl alloys, such as Ag-Cu [12], Ti-Ni [13], Ti-Ni-Si [14], have high melting points (> 1050 K) and cannot be applied in this case. He et al. [15] and Shiue et al. [16] respectively brazed the C_f/Al as well as the TiAl using Al-based filler metal (melting points of 773–850 K). However, the brittle reaction products associated with the process seriously deteriorate the joint properties. Moreover, previous studies [17–20] indicate that the C_f/Al composites are temperature-sensitive. Long-time heat treatment above 823 K leads to an interfacial chemical reaction between the aluminum matrix and carbon fibers. In addition, large pressure variations lead to crack formation in the carbon fiber/aluminum matrix interface zone. Consequently, these constrains preclude use of the conventional joining methods, such as fusion welding, diffusion bonding, brazing etc. [21]. Therefore, developing a successful method for joining TiAl alloys and C_f/Al composites is a challenging and demanding task.

Exothermic joining, which involves integrated or self-propagating, exothermic chemical reactions when ignited [22], is an efficient technique for joining dissimilar materials [23]. Since the released reaction heat localizes at the interfaces during the joining, temperature-sensitive materials can be joined without thermal damage [24]. Products with desired properties can also be synthesized in-situ and serve as a gradient layer to relieve joint stresses [25]. Thus far the majority of researches in exothermic joining has been focused on high-temperature materials, such as ceramics [26], superalloys [27], intermetallics [28]. However, there has been little discussion regarding the joining of TiAl alloys and C_f/Al composites.

In this work, TiAl alloys and C_f/Al composites were joined by the exothermic reaction of the Ni-Al interlayer. The interlayer was doped with various amounts of Ti. To further increase the joining efficiency and to decrease the energy consumption, a continuous wave laser beam was used to ignite the interlayer. The effect of Ti addition on the joint microstructures and mechanical properties was systematically investigated. Finally, a proposed joint formation mechanism is discussed.

2. Experimental procedure

The C_f/Al composites considered in this study had a fiber volume fraction of 50% in a 6061 aluminum matrix. The TiAl alloy had a nominal composition of Ti-48Al-7V-0.3Y (at.%) and a melting point of ~1750 K. Due to an addition of Vanadium and Yttrium, the TiAl alloys consisted of γ, B_2, and YAl_x phases. The microstructures of C_f/Al and TiAl substrates are depicted in Fig. 1. Before joining, the C_f/Al and TiAl substrates were cut into 5 mm × 5 mm × 3 mm and 12 mm × 8 mm × 2 mm specimens, respectively. The mating surfaces were polished with SiC paper up to grit 1000. Cleaning was performed ultrasonically in acetone for 15 min.

Commercial powders (Beijing Xing Rong Yuan Technology Co., Let., China) of high purity Ni (D_{90} ≈ 45 μm, purity 99.5%), Al (D_{90} ≈ 45 μm, purity 99.5%) and Ti (D_{90} ≈ 25 μm, purity 99.5%) were used for interlayers in this study. Appropriate amounts of powders were weighed out and milled in an agate bowl using Al_2O_3 balls. The diameters of the balls were 5 mm and 10 mm respectively. Milling was performed for 1 h in argon with the rotation speed of 300 rpm. The weight ratio of Al_2O_3 ball to powders was 10:1. A 0.5 g sample of the milled powders were uniaxially cold-pressed into a cylindrical shape of 10 mm diameter and about 1.3 mm long. The green density of powder compact was about 90% of the theoretical density under the pressure force of 50 kN.

The joining was performed in an inert, argon atmosphere. A Ytterbium Fiber Laser (YLR-100-AC, beam power of 100 W, beam diameter of 0.2 mm) was used to ignite the powder compacts. Firstly, the compacts were ignited individually to measure their real reaction temperatures. Laser beam heated the compacts for 1 s and resulted in ignition. The time-temperature data was simultaneously achieved using a fine-wire (300 μm) Pt/Pt-13%Rh thermocouple, which was inserted into the center of the powder compacts. Then, the powder compact was sandwiched between the substrates under 2–3 MPa. Laser beam heated the compact for 5 s, resulting in ignition and subsequent propagation of the exothermic reaction front through the composite, to create the joint. Fig. 2 shows the schematic of the joining procedure.

To characterize the joint microstructure, cross-sectioned samples were prepared for SEM and polished using 1 μm diamond polishing spray. The specimens, after joining, were milled within the interface domain by using a Focused Ion Beam (FIB) (Helios Nanolab600i, FEI Co., Ltd., USA) system for TEM observation. The samples were characterized by scanning electron microscopy (SEM, Helios Nanolab600i, FEI Co., Ltd., USA) equipped with energy dispersive spectrometer (EDS), X-ray diffraction (XRD, D8 ADVANCE) and transmission electron microscopy (TEM, Talos F200X, FEI Co., Ltd., USA). The joint shear strength at room temperature was examined using the universal testing machine (INSTRON 5569, USA) at a shear rate of 0.5 mm·min^{-1}.

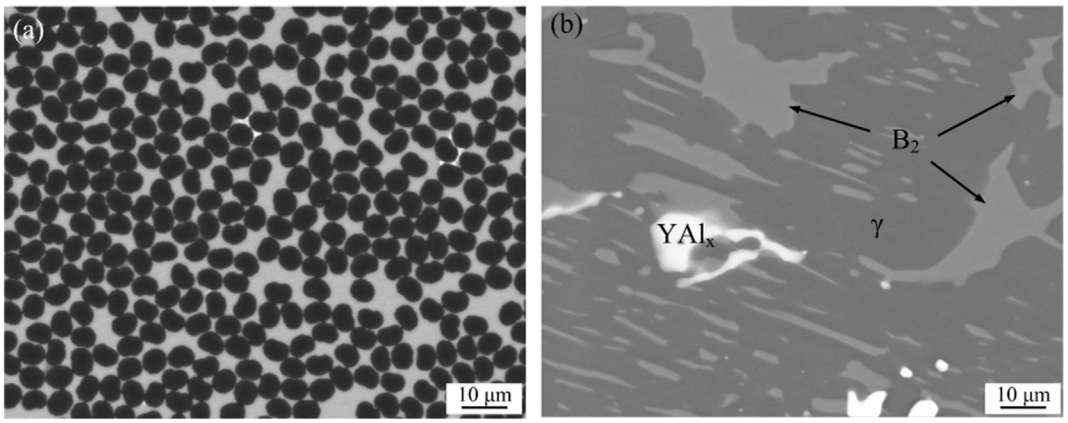

Fig. 1. Microstructures of the substrates: (a) C_f/Al; (b) TiAl.

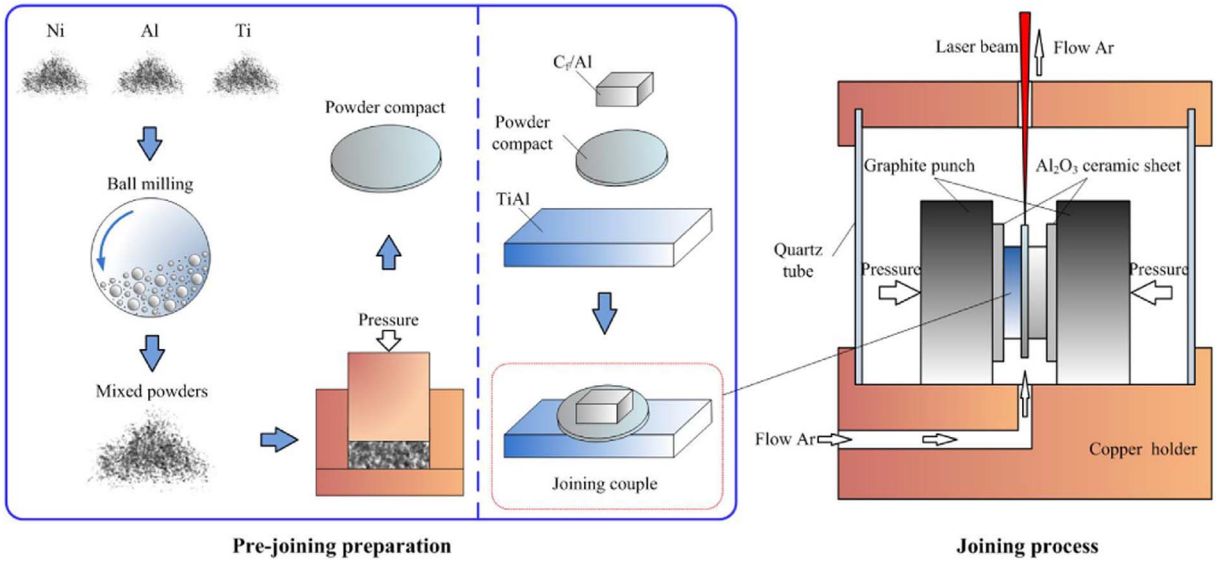

Fig. 2. Schematic of the joining procedure.

3. Results and discussion

3.1. Adiabatic temperature calculation

In exothermic joining [10,29], the exothermic reaction in the interlayer serves as the only heat resource except for necessary igniting power. The commonly used exothermic interlayers are divided into two kinds: (i) an interlayer consisting of an active metal (Ti or Zr), and a nonmetal with a small atomic diameter (C, B or B_4C) [30], and (ii) an interlayer consisting of mixed metals (Ti + Al [31,32], Zr + Al [33] or Ni + Al [34,35]). Among those exothermic reaction systems, the equimolar Ni-Al system shows both a heat-release and a high reaction rate. For these reasons, it is selected as the joining interlayer in this study. However, the reaction products of Ni-Al interlayer have a poor wettability on the carbon fibers, which would lead to weak bonding at the C_f/interlayer products interface [10]. The high volume fraction (50%) of C_f in the C_f/Al composites would increase the weak bonding area in the joint and exacerbate this effect. Previous studies [29,34] indicate that active elements (Ti, for example) are indispensable in a successful joining of carbon materials since they can improve the poor wettability of filler metals on carbon. Therefore, to enhance the affinity of the interlayer products and the carbon fibers, a small amount of Ti (the strong carbide-forming element) should also be added to the interlayer.

The joining process is a result of complex chemical reactions and the bonding result is highly temperature dependent. The adiabatic temperature (T_{ad}), i.e., the theoretical reaction temperature achieved under adiabatic condition, offers a useful metric of the reaction system. Specifically, the T_{ad} can be determined by solving the following equation [36]:

$$-\Delta H_{298}^{\Theta} = \int_{298}^{T_{ad}} c(T)dT \tag{1}$$

where $\Delta H_{298}{}^{\Theta}$ is the enthalpy change of the reaction, and $c(T)$ is the specific heat of the reaction products as a function of temperature.

The adiabatic temperature of the interlayers with different Ti content was calculated using Eq. (1). To simplify the calculation, the addition of Ti was considered as the diluent. The evaluated adiabatic temperature curve is represented in Fig. 3. The trend obtained indicates a change with the increase of Ti content. When the Ti content ranges from 0 to 21.46 wt.%, the T_{ad} appears to be independent of Ti content, thus has a constant value of 1912 K (the T_{ad} of equimolar Ni-Al system). This could be explained by the volume change of the liquid phase in the reaction products. When the Ti content was 0, the reaction products were NiAl intermetallics (with a melting point of 1912 K) in the solid-liquid coexistence state. The addition of Ti absorbs a certain amount of thermal energy and decreased the volume fraction of liquid NiAl intermetallics in the reaction products. Hence, the adiabatic temperature stabilizes at the melting point (1912 K) until the melting rate

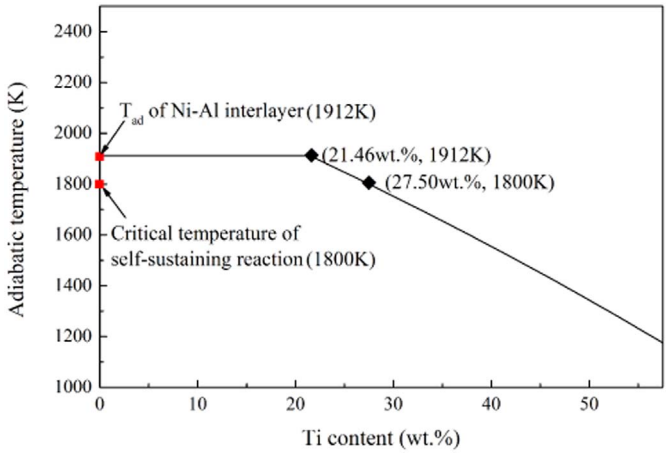

Fig. 3. Adiabatic temperature of the interlayer vs. Ti content.

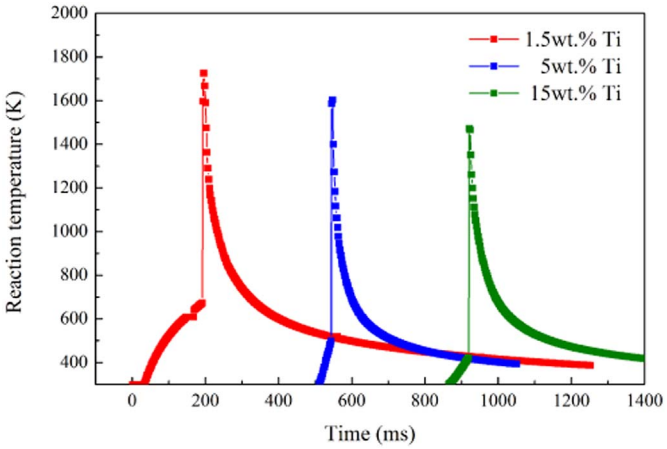

Fig. 4. Measured reaction temperatures of the interlayers with different Ti content.

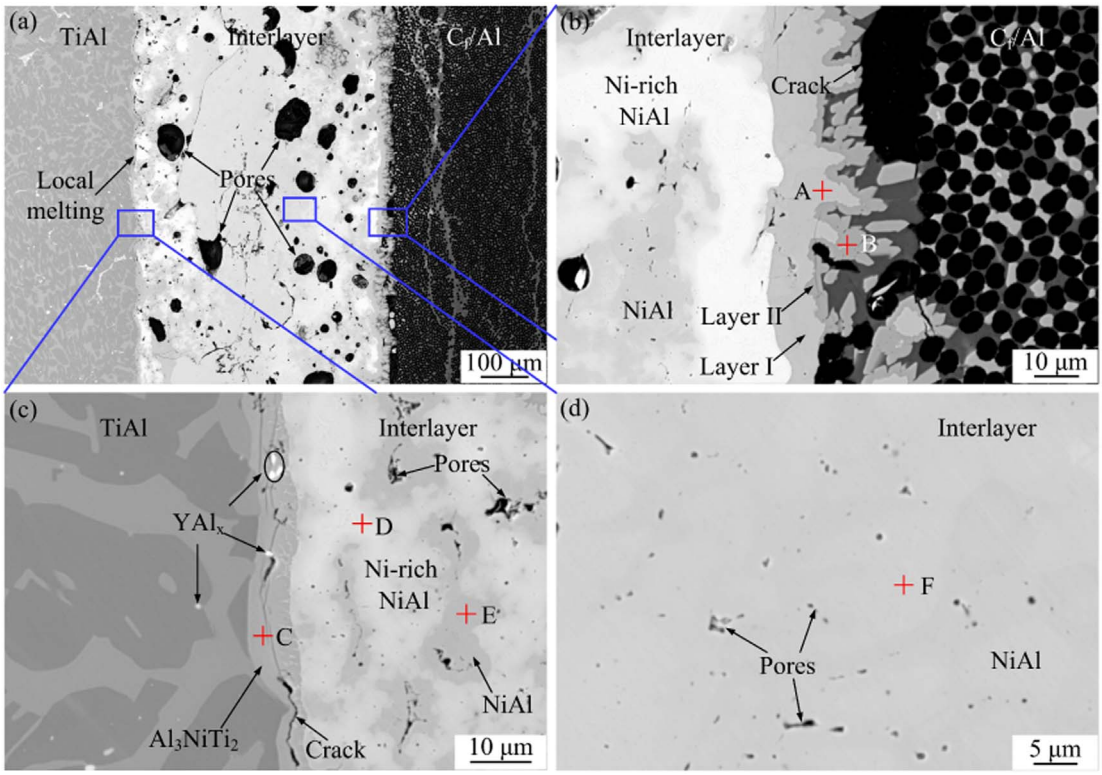

Fig. 5. Microstructure of the TiAl-C_f/Al joint with Ni-Al interlayer. (a) Overall view; (b) on the C_f/Al side; (c) on the TiAl side; (d) in the interlayer.

decreases to 0 (the corresponding Ti content is 21.46 wt.%). Subsequently, the T_{ad} gradually decreases with a further increase of Ti content.

For a self-sustaining exothermic reaction, a theoretical adiabatic temperature of 1800 K is often considered as the empirical lower limit [37]. Additionally, the reaction is also expected to yield large quantity of liquid, hence eliminating the formation of pores in the final reaction products synthesis [10,22,38]. Therefore, the ideal adiabatic temperature for this interlayer should achieve melting point of NiAl intermetallics (1912 K). The products are then in the liquid-solid state and easy-to-densify. Correspondingly, the best Ti content in the reaction system was determined to be within the range of 0–21.5 wt.%. The measured reaction temperatures of the interlayers with different Ti content is shown in Fig. 4. Data indicate that the reaction temperature experiences a slight decrease with the increase of the Ti content, as predicted, because the higher Ti content decreases the volume of the liquid phase in the products, hence lowering the exothermicity. Furthermore heat losses will inevitably lead to temperatures lower than the adiabatic temperature.

3.2. Microstructure of the TiAl-C_f/Al joints

The TiAl alloys and C_f/Al composites were joined using the Ni-Al interlayer. The interfacial microstructure of the TiAl-C_f/Al joint is illustrated in Fig. 5. One can conclude that the reaction in the interlayer was complete, without any residual Ni or Al particles. Continuous cracks and a large quantity of pores were detected in the joint domain. To check the phase composition, various locations, as indicated in Fig. 5(b)–(d), were selected for EDS measurements. Corresponding EDS spectrums are shown in Fig. 6. Results in Table 1 show that the ratio of Ni and Al at the location of points E and F is close to 1:1. To further identify the phase composition, a XRD analysis was carried out. The C_f/Al substrate was removed by grinding until the interlayer products were reached, and then subjected to XRD procedure. Fig. 7(a) reveals that the NiAl phase is formed. The peaks appearing at $2\theta = 30.95^\circ$, 44.34°, 55.04°, 64.49° and 81.60° could be respectively confirmed as (100), (110), (111), (200) and (211) of the NiAl phase, in accordance with the standard JCPDS card (No. 44-1188) of the cubic NiAl [39].

On the C_f/Al side, the interlayer products reacted with the aluminum matrix, forming two distinct reaction layers: layer I (see the location of the point A, 10 μm thick) and layer II (see the location of the point B, 4 μm thick). These layers were considered as the Ni_2Al_3 and $NiAl_3$, respectively. They had the Ni:Al atomic ratios approaching 2:3 and 1:3. One 8 μm width gray layer (see the location of point C) was observed near the TiAl substrate. The atomic ratio of Ni, Al and Ti was close to 1:3:2. It is established that during a shear test, some joints may fracture within this layer. The XRD pattern of the fractured surface (see Fig. 7(b)) indicates a mixture of NiAl and Al_3NiTi_2 phases. The detected NiAl phase is most likely related to interlayer products since the fracture surfaces are irregular and may propagate into the joint center. Thus, this gray layer should be the Al_3NiTi_2 phase with the $MgZn_2$-type lattice structure [40]. The formation of Al_3TiNi_2 layer was also reported by Liu et al. [41] for a system involving joining the TiAl intermetallics and Ti_3AlC_2 ceramic.

Analysis in Section 3.1 shows that the exothermic reaction of Ni-Al interlayer can produce high temperature from the alloying reaction ($Ni + Al = NiAl$, $\Delta H^0 = -118.41\ kJ{\cdot}mol^{-1}$). Under this condition, the adjacent mating substrates locally melt. Some bright phases were observed near the substrates in Fig. 5(b) and (c). The EDS results indicate that the Ni content of these phases (point D, 60.33Ni (at.%), 39.67Al (at.%)) was higher than NiAl phase (point F, 49.4 Ni (at.%), 50.6 Al (at.%)). These phases were confirmed as the Ni-rich NiAl phases according to previous work [3]. Their formation is hypothesized as follows. During the joining, heat is lost to the substrates [24], such that the temperature at the interlayer/substrate interface is lower than the center of the interlayer. There is not enough time for the Ni, Al atoms in the NiAl phase to homogenize completely, forming the Ni-rich NiAl phases (point D) on two sides. In addition, the Ni-Al products have a poor wettability on the carbon fibers [3]. Under the rapid heating and subsequent cooling, a large thermal stress is produced at the interlayer/

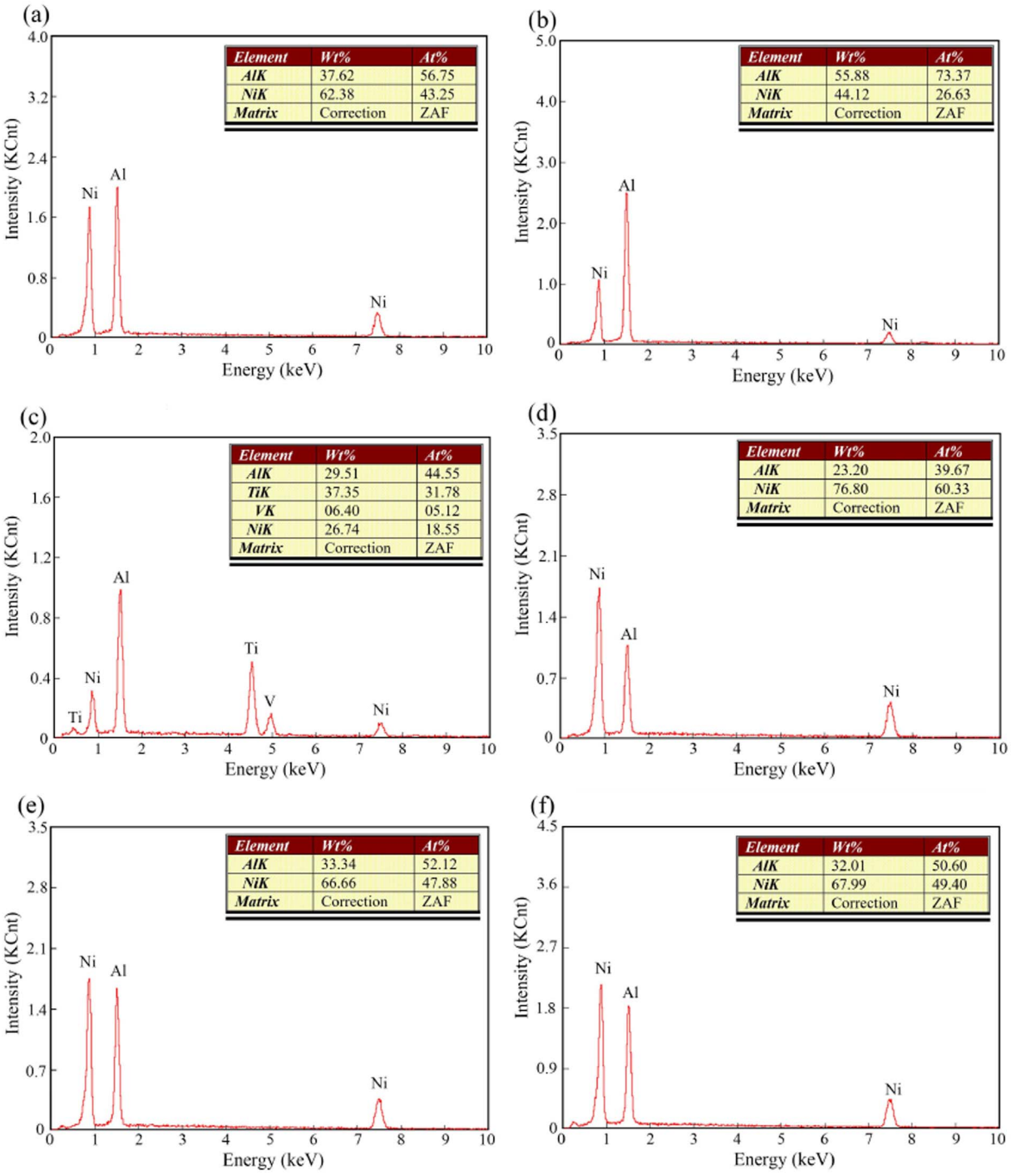

Fig. 6. (a)–(f) EDS spectrum of points A–F in Fig. 5, respectively.

Table 1
EDS results of the joint of Fig. 5.

Point	Elements (at.%)				Possible phase
	Ni	Al	Ti	V	
A	43.25	56.75	/	/	Ni_2Al_3
B	26.63	73.37	/	/	$NiAl_3$
C	18.55	44.55	31.78	5.12	Al_3NiTi_2
D	60.33	39.67	/	/	Ni-rich NiAl
E	47.88	52.12	/	/	NiAl
F	49.4	50.6	/	/	NiAl

substrate interface, leading to an appearance of continuous cracks on both sides of the joint zone (see Fig. 5(b) and (c)).

Fig. 8 presents the microstructure of the TiAl-C_f/Al joint with Ni-Al-Ti interlayer and indicates that the joint domain underwent a dramatic change. Defects such as the large pores and continuous cracks visible in Fig. 5, have disappeared. The interlayer products containing the light gray block phase and gray reticular phase were dense. They feature a eutectic appearance (see Fig. 8(d)) and are well bonded with the substrates (see Fig. 8(b) and (c)).

The interlayer/carbon fiber and interlayer/TiAl interfaces, marked by the red rectangles in Fig. 8(b) and (c), were examined by the Transmission Electron Microscopy (TEM). The typical bright field (BF) images of selected zones are illustrated in Fig. 9(a) and (b). Data show

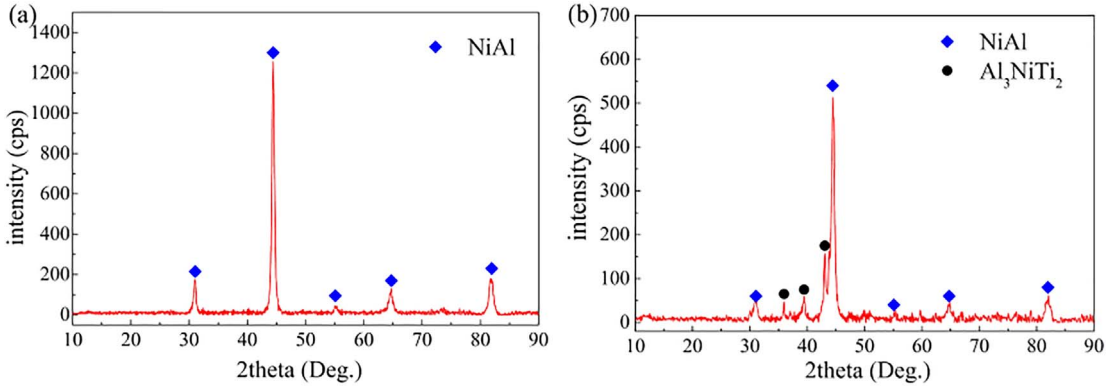

Fig. 7. XRD results of (a) the interlayer products and (b) the fracture surface.

that between the carbon fiber and the $NiAl_3$ layer, a 300–400 nm thick Ti-C reaction layer exists. The nanoscale dark particles precipitated out within this layer and were identified as the TiC phase according to the selected area electron diffraction (SAED) data in Fig. 9(c). Thermodynamic calculations reveal that the Gibbs free energy change of Ti + C → TiC has a large negative value ($\Delta G^0 = -180.48$ kJ·mol^{-1}). The formation of this Ti-C layer is a spontaneous process. It improved the wettability of the interlayer products on the carbon fibers and played a key role in the good bonding [3,34].

Fig. 9(b) shows that the reaction layer on the TiAl side extends to the interlayer and forms the eutectic with the block NiAl. The SEAD in Fig. 9(e) reveals that this reaction layer was identified as the Al_3NiTi_2, and had the same composition and lattice structure with the gray reticular phase in the eutectic. Thus, the interlayer products were confirmed as the NiAl + Al_3NiTi_2 eutectic. Generally, the eutectic has a lower melting temperature [42]. A lower melting temperature increases the processability of the materials, due to a better fluidity [43]. Hence, the interface products appear to densify under the same pressure easier. As a result, the joint density is highly improved. Meanwhile, the addition of Ti also tempered the violent exothermic reaction of Ni-Al interlayer. The thermal stress in the interfaces decreased effectively. The disappearance of the micro cracks in the Al_3NiTi_2 reaction layer, see Fig. 8(c), indicates more favorable thermal stresses at the interface.

3.3. Formation mechanism of the TiAl-C_f/Al joint

Based on the performed analysis, it may be concluded that the addition of Ti plays a key role in a successful joining of TiAl alloys and C_f/Al composites. In order to illustrate the evolution of key phenomena occurring during the joining process, a physical model was established. The schematic illustration is offered in Fig. 10.

The formation of the TiAl-C_f/Al joint was divided into the following stages:

1) Ignition of the interlayer. Prior to the joining, the interlayer was sandwiched between the substrates under pressure, to assure sufficient contact with the interlayer. Ignition is localized, and the heat is not so readily dispersed due to the porous nature of the

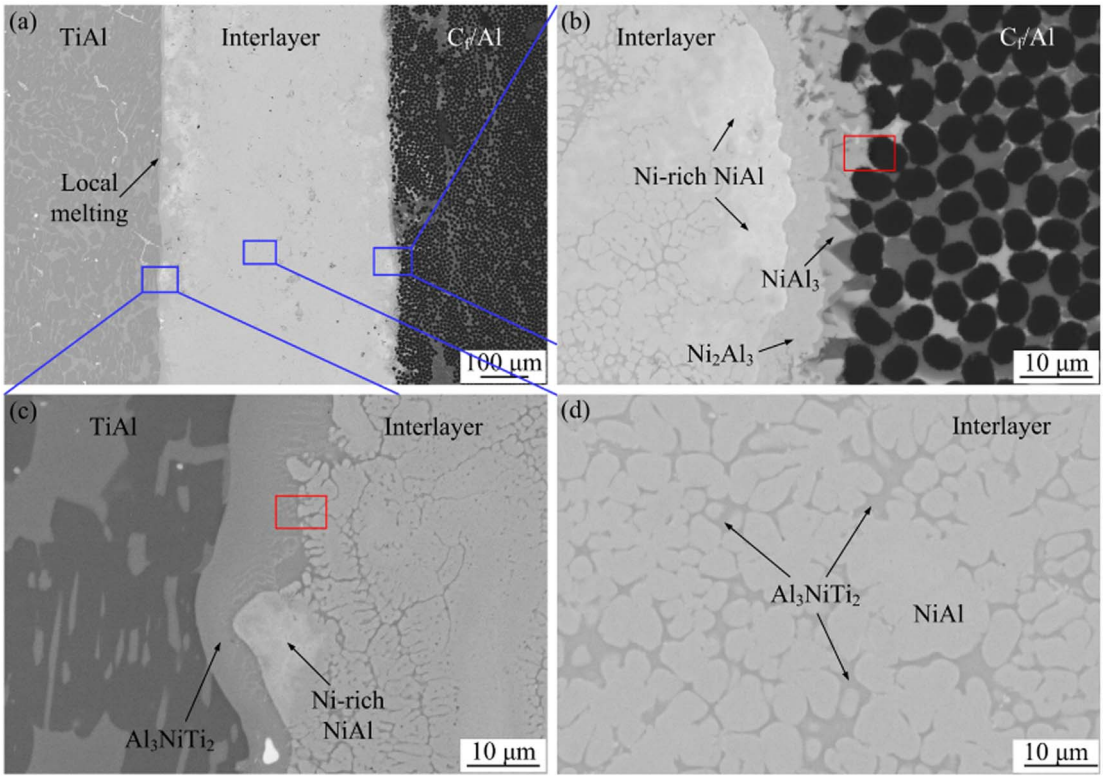

Fig. 8. Microstructure of the TiAl-C_f/Al joint with Ni-Al-Ti interlayer. (a) Overall view; (b) on the C_f/Al side; (c) on the TiAl side; (d) in the interlayer.

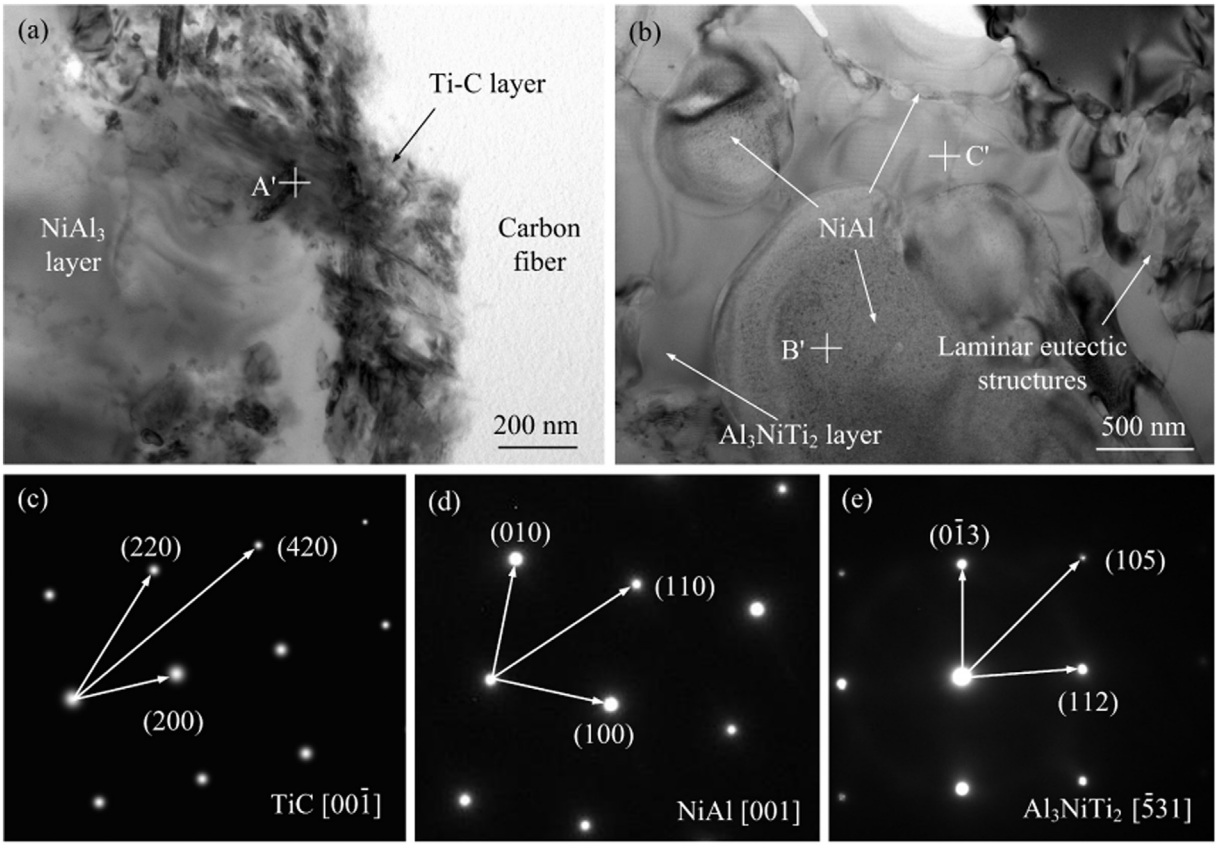

Fig. 9. TEM micrographs of (a) the $NiAl_3/C_f$ and (b) reaction layer/TiAl interfaces respectively; SAED patterns of (c) point A', (d) B' and (e) C'.

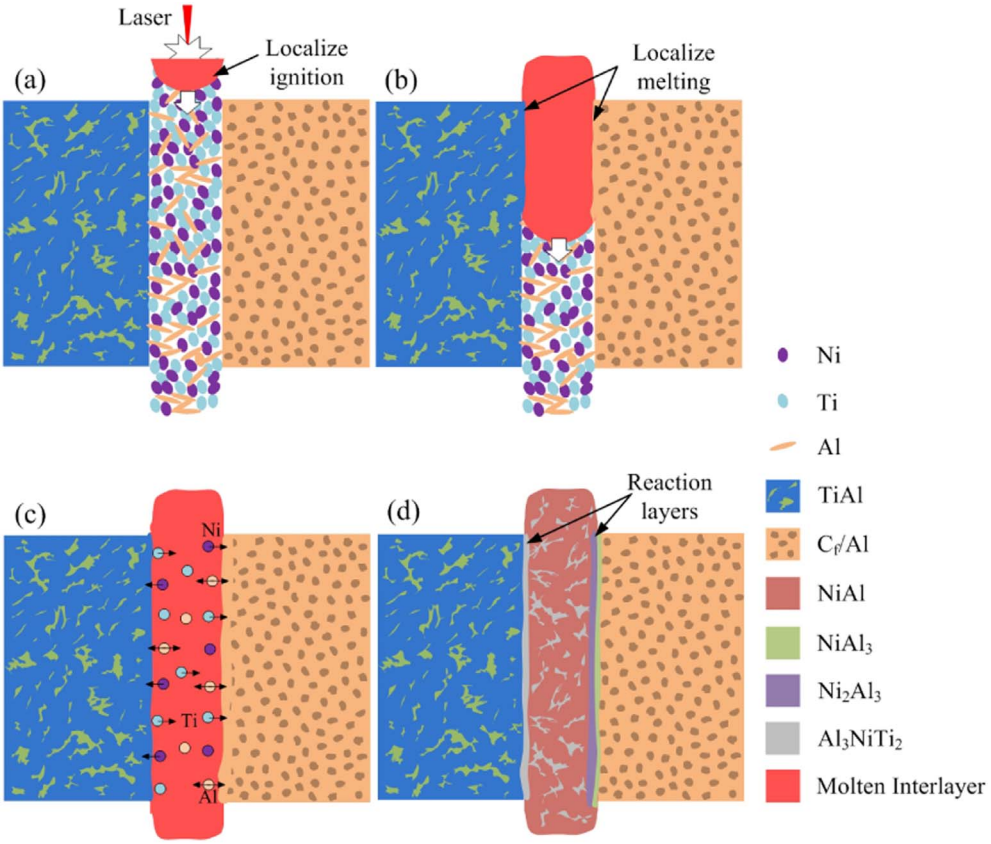

Fig. 10. Formation of the TiAl-C_f/Al joint. (a) Ignition of the interlayer; (b) propagation of the reaction front; (c) atomic exchange; (d) formation of the joint.

powder compact [22]. The temperature of this area reached the melting point of Al rapidly. Molten aluminum fills the pores under capillary forces and increases the contact between Ni, Ti and Al. Exothermic reactions (Ni(s) + Al(l) → $NiAl_3$, Ti(s) + Al(l) → $TiAl_3$) then occurred in the Al/Ni and Al/Ti interface, leading to a localized ignition in the interlayer, see Fig. 10(a). The chemical reactions that occur during ignition have been investigated in our previous study [21], thus are not discussed here.

2) Propagation of the exothermic reaction front. Upon ignition of the interlayer, the heat generated from the exothermic reaction quickly dissipates into the interlayer owing to the high thermal conductivity of Aluminum and Nickel. This results in heating the adjacent region to its ignition temperature, leading to a self-sustained reaction. The reaction temperatures of interlayer when ignited individually were measured as 1471 K–1724 K with different Ti, as shown in Section 3.1. During the reaction, the interlayer products are in a liquid-solid state. Since both the reactants before reaction and partial interlayer products after reaction were in the solid state, this exothermic reaction front has been considered a solid flame [44], which propagates within the interlayer. The heat from the exothermic reaction and laser beam induces a localized melting in the substrate, as shown in Fig. 10(b).
3) Atomic exchange. During/after the exothermic reaction, the interlayer products are in a solid-liquid state with the substrates undergoes a localized melting. The regions in the liquid phase greatly enhanced the atom mobility, including diffusion and advection. Ni, Ti and Al atoms migrated through the substrates/interlayer interfaces owing to their concentration gradient, as shown in Fig. 10(c). Meanwhile, considering the high affinity of Ti and C, as well as the formed Ti-C reaction layer, Fig. 9(a), it is logical to deduce that the Ti content would feature a concentration change around the carbon fibers.
4) Formation of the joint. During and upon cooling, heat is transferred from the interlayer products to the substrates and ultimately to the surrounding environment. Solidification first occurs within the region adjacent to the substrates. On the TiAl side, Ni, Ti, Al atoms bond with each other following the reaction paths: Ni + Al + Ti → Al_3NiTi_2. On the C_f/Al side, $NiAl_3$ and Ni_2Al_3 reaction layers form due to the reaction: Ni + Al → $NiAl_3$, Ni + $NiAl_3$ → Ni_2Al_3. Meanwhile, Ti atoms diffuse towards the composites. Due to a low content of Ti in the interlayer, and a high affinity of Ti and C (Ti + C → TiC, $\Delta G^0 = -180.48\ kJ{\cdot}mol^{-1}$), elemental Ti concentrates in the region around the carbon fibers, forming a Ti-C layer. This Ti-C layer greatly enhances the wettability of the interlayer products on the carbon fibers [29,34]. In the interlayer, the NiAl and Al_3NiTi_2 precipitate from the Ni-Al-Ti melt. As the temperature

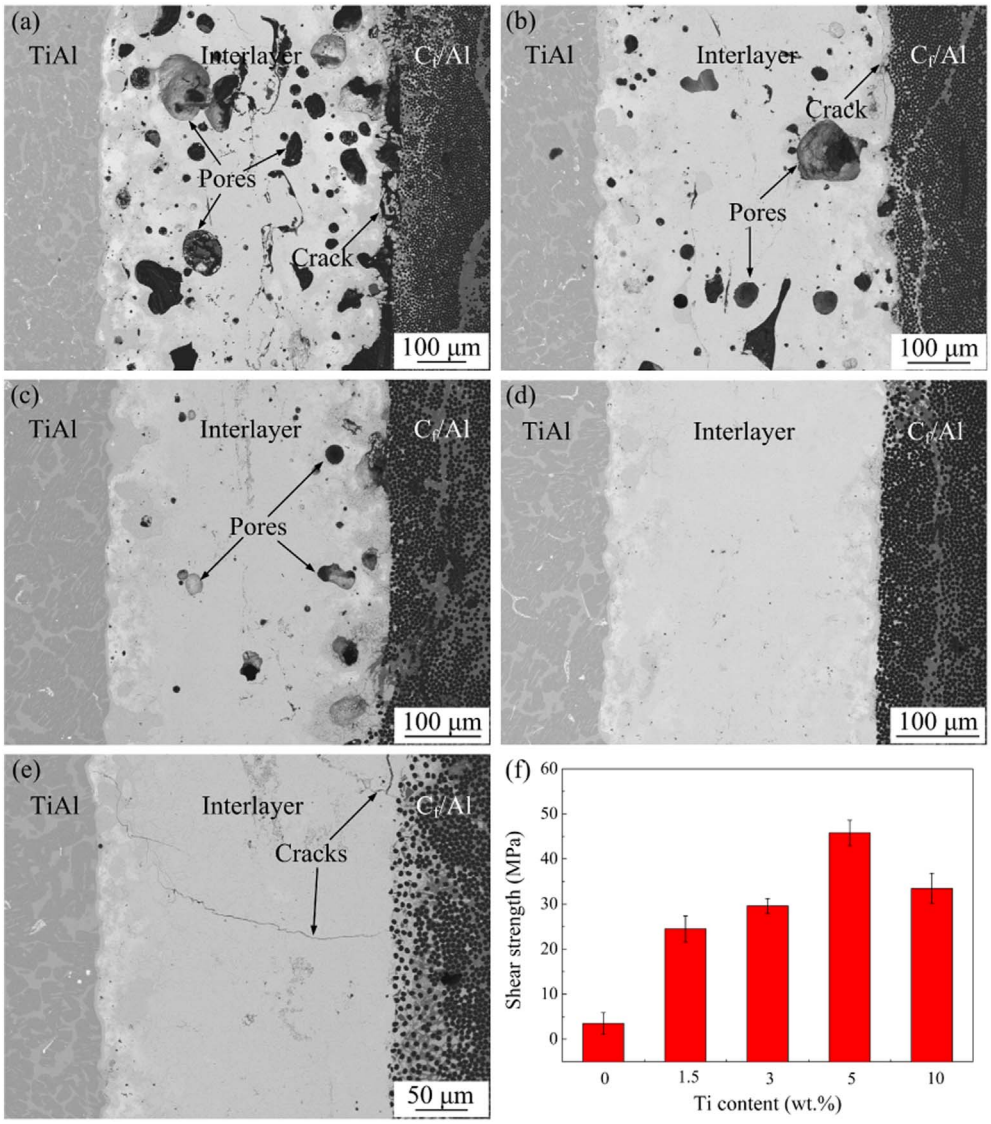

Fig. 11. (a)–(e) Microstructures of the joints with the Ti content of 0 wt.%, 1.5 wt.%, 3 wt.%, 5 wt.%, 10 wt.%, respectively; (f) joint shear strength.

decreases, the atomic diffusion in the joint domain gradually reduces, the liquid phases disappear, forming the final joint, as shown in Fig. 10(d).

3.4. Effect of Ti content on the joint microstructure and the shear strength

Fig. 11(a)–(e) shows the microstructures of the TiAl-C_f/Al joints with different Ti content. With the increase of Ti content, the joint morphology features changes. It is apparent that both the population of pores and their size decrease significantly. The cracks in the joint first gradually disappear as the Ti content increases to 5 wt.%, just to emerge again when the Ti content gets to the 10 wt.% level. The reason of these changes is that variation of Ti content leads to different interlayer products and influences the interfacial reactions. As analyzed in Section 3.2, the products of the Ni-Al-Ti interlayer constitute the NiAl + Al_3NiTi_2 eutectic. Higher Ti content correspondingly increases the proportion of the eutectic in the interlayer products and lowers the melting point. During the joining, the interlayer products could have a better fluidity. The original pores in the powder interlayer would be eliminated more easily, leading to the elevation of the joint density.

The increase of Ti content also greatly improves the bonding quality on both sides. Due to the great affinity of Ti and C (Ti + C → TiC, $\Delta G^0 = -180.48\ \mathrm{kJ{\cdot}mol^{-1}}$), a nano-scale Ti-C reaction layer forms on the carbon fiber/interlayer interface. This Ti-C reaction layer effectively enhances the interfacial reaction between the interlayer products and the carbon fibers. Higher Ti content in the interlayer promotes this process, hence improves the bonding quality on the C_f/Al side. As a result, the unconnected areas on the C_f/Al side gradually disappear, see Fig. 11(a)–(e). Furthermore, an increase of Ti content tempers a violent exothermic reaction of the Ni-Al interlayer (see the temperature histories in Fig. 4). Consequently, the thermal stress in the joint is reduced. However, a further increase of the Ti content leads to an excess of Al_3NiTi_2 making the interlayer products brittle due to the hardening of the NiAl matrix and the segregation of the Al_3NiTi_2 at NiAl grain boundaries [45]. When the Ti content increases to 10 wt.%, continuous cracks emerge again.

Shear strength testing has been performed at room temperature to establish the mechanical properties of different TiAl-C_f/Al joints and the corresponding results are presented in Fig. 11(f). The change of shear strength is well dependent on the joint microstructure evolution in Fig. 11(a)–(e). When the Ti content is 0 wt.%, large pores and continuous cracks form in the joint. The joint can not suffer high shear force and only had a low shear strength of 3.48 MPa. As the Ti content increases, pores and cracks gradually disappear in the joint domain. As a result, the shear strength firstly gradually increases until the maximum shear strength of 45.8 MPa is reached when the Ti content is 5 wt.%. The further increase of the Ti content enhances the interfacial reactions but embrittles the interlayer products. Cracks emerge again in the joint, leading to the following drop of the shear strength.

4. Conclusions

A method for bonding Carbon Fiber (C_f)/Al composites and TiAl alloys was developed by means of laser-induced exothermic reaction of a Ni-Al-Ti interlayer. The adiabatic temperature was calculated, and the Ti content (0–21.5 wt.%) in the reaction system was determined. The addition of Ti played a key role in a successful joining. It transformed the interlayer products from NiAl to NiAl + Al_3NiTi_2 eutectic, and enhanced the interfacial reaction between carbon fiber and interlayer products by forming a thin Ti-C layer at the $NiAl_3$/carbon fiber interface. The typical interfacial structure of the joint was identified as (C_f/Al)/Ti-C/$NiAl_3$/Ni_2Al_3/(NiAl + Al_3NiTi_2)/Al_3NiTi_2/TiAl. The sequence of stages of the joint formation was further discussed. Finally, the effect of Ti content on the microstructure and mechanical properties of joints were investigated in detail. The optimum value of Ti content was found to be 5 wt.%, which led to a defect-free joint and a maximum shear strength of 45.8 MPa.

Acknowledgements

The authors gratefully acknowledge the financial support from the National Natural Science Foundation of China under Grant no. 51075101. DPS acknowledges the support through the Distinguished 1000 Plan Foreign Professor appointment at the Harbin Institute of Technology, PR China.

References

[1] R.H. Baughman, A.A. Zakhidov, W.A. De Heer, Carbon nanotubes—the route toward applications, Science 297 (2002) 787–792.
[2] E.T. Thostenson, Z. Ren, T.-W. Chou, Advances in the science and technology of carbon nanotubes and their composites: a review, Compos. Sci. Technol. 61 (2001) 1899–1912.
[3] W. Zhou, G. Yamamoto, Y. Fan, H. Kwon, T. Hashida, A. Kawasaki, In-situ characterization of interfacial shear strength in multi-walled carbon nanotube reinforced aluminum matrix composites, Carbon 106 (2016) 37–47.
[4] G.-J. Feng, Z.-R. Li, R.-H. Liu, S.-C. Feng, Effects of joining conditions on microstructure and mechanical properties of C_f/Al composites and TiAl alloy combustion synthesis joints, Acta Metall. Sin. (Engl. Lett.) 28 (2015) 405–413.
[5] A. Pai, S.S. Sharma, R.E. D'Silva, R.G. Nikhil, Effect of graphite and granite dust particulates as micro-fillers on tribological performance of Al 6061-T6 hybrid composites, Tribol. Int. 92 (2015) 462–471.
[6] M. Velamati, E. Aguilar, M.A. Garza-Castañon, N.P. Hung, M. Powers, Laser and resistance joining of aluminum–graphite composite, J. Mater. Process. Technol. 212 (2012) 2549–2557.
[7] M.-K. Tang, X.-J. Huang, J.-G. Yu, X.-W. Li, Q.-X. Zhang, Simple fabrication of large-area corrosion resistant superhydrophobic surface with high mechanical strength property on TiAl-based composite, J. Mater. Process. Technol. 239 (2017) 178–186.
[8] G. Feng, Z. Li, S. Feng, Z. Shen, Effect of Ti–Al content on microstructure and mechanical properties of C_f/Al and TiAl joint by laser ignited self-propagating high-temperature synthesis, Trans. Nonferrous Metals Soc. China 25 (2015) 1468–1477.
[9] L. Song, J. Lin, J. Li, Effects of trace alloying elements on the phase transformation behaviors of ordered ω phases in high Nb-TiAl alloys, Mater. Des. 113 (2017) 47–53.
[10] G. Feng, Z. Li, Z. Zhou, Y. Wang, Joining of C_f/Al composites and TiAl intermetallics by laser-induced self-propagating high-temperature synthesis using the Ni-Al-Zr interlayer, Mater. Des. 110 (2016) 130–137.
[11] X. Chen, R. Xie, Z. Lai, L. Liu, G. Zou, J. Yan, Ultrasonic-assisted brazing of Al–Ti dissimilar alloy by a filler metal with a large semi-solid temperature range, Mater. Des. 95 (2016) 296–305.
[12] J. Feng, X. Dai, D. Wang, R. Li, J. Cao, Microstructure evolution and mechanical properties of ZrO_2/TiAl joints vacuum brazed by Ag–Cu filler metal, Mater. Sci. Eng. A 639 (2015) 739–746.
[13] X. Song, B. Ben, S. Hu, J. Feng, D. Tang, Vacuum brazing high Nb-containing TiAl alloy to Ti60 alloy using Ti-28Ni eutectic brazing alloy, J. Alloys Compd. 692 (2017) 485–491.
[14] J. Cao, P. He, M. Wang, Mechanical milling of Ti–Ni–Si filler metal for brazing TiAl intermetallics, Intermetallics 19 (2011) 855–859.
[15] P. He, Y.Z. Liu, D. Liu, Interfacial microstructure and forming mechanism of brazing C_f/Al composite with Al-Si filler, Mater. Sci. Eng. A 422 (2006) 333–338.
[16] R.K. Shiue, S.K. Wu, S.Y. Chen, Infrared brazing of TiAl using Al-based braze alloys, Intermetallics 11 (2003) 661–671.
[17] I. Alfonso, O. Navarro, J. Vargas, A. Beltrán, C. Aguilar, G. González, I.A. Figueroa, FEA evaluation of the Al_4C_3 formation effect on the Young's modulus of carbon nanotube reinforced aluminum matrix composites, Compos. Struct. 127 (2015) 420–425.
[18] R. Deaquino-Lara, N. Soltani, A. Bahrami, E. Gutiérrez-Castañeda, E. García-Sánchez, M.A.L. Hernandez-Rodríguez, Tribological characterization of Al7075-graphite composites fabricated by mechanical alloying and hot extrusion, Mater. Des. 67 (2015) 224–231.
[19] M. Lee, Y. Choi, K. Sugio, K. Matsugi, G. Sasaki, Effect of aluminum carbide on thermal conductivity of the unidirectional CF/Al composites fabricated by low pressure infiltration process, Compos. Sci. Technol. 97 (2014) 1–5.
[20] S.P. Rawal, Interface structure in graphite-fiber-reinforcedmetal-matrix composites, Surf. Interface Anal. 31 (2001) 692–700.
[21] G.-J. Feng, Z.-R. Li, S.-C. Feng, W.-J. Zhang, Microstructure evolution and formation mechanism of laser ignited SHS joining between C_f/Al composites and TiAl alloys with Ni-Al-Ti interlayer, Rare Metals (2015), http://dx.doi.org/10.1007/s12598-015-0542-1.
[22] A.E. Sytschev, D. Vrel, O.D. Boyarchenko, D.V. Roshchupkin, N.V. Sachkova, Combustion synthesis in bi-layered (Ti − Al)/(Ni − Al) system, J. Mater. Process. Technol. 240 (2017) 60–67.
[23] A.G. Merzhanov, I.P. Borovinskaya, Self-propagating high-temperature synthesis of refractory inorganic compounds, Dokl. Akad. Nauk SSSR 204 (1972) 366–369.
[24] T. Fiedler, I.V. Belova, S. Broxtermann, G.E. Murch, A thermal analysis on self-propagating high temperature synthesis in joining technology, Comput. Mater. Sci. 53 (2012) 251–257.
[25] Z. Li, G. Feng, S. Wang, S. Feng, High-efficiency joining of C_f/Al composites and

TiAl alloys under the heat effect of laser-ignited self-propagating high-temperature synthesis, J. Mater. Sci. Technol. 32 (2016) 1111–1116.
[26] R. Rosa, P. Veronesi, S. Han, V. Casalegno, M. Salvo, E. Colombini, C. Leonelli, M. Ferraris, Microwave assisted combustion synthesis in the system Ti-Si-C for the joining of SiC: experimental and numerical simulation results, J. Eur. Ceram. Soc. 33 (2013) 1707–1719.
[27] C. Pascal, R.M. Marin-Ayral, J.C. Tèdenac, Joining of nickel monoaluminide to a superalloy substrate by high pressure self-propagating high-temperature synthesis, J. Alloys Compd. 337 (2002) 221–225.
[28] J.C. Feng, J. Cao, Z.R. Li, Microstructure evolution and reaction mechanism during reactive joining of TiAl intermetallic to TiC cermet using Ti-Al-C-Ni interlayer, J. Alloys Compd. 436 (2007) 298–302.
[29] J. Cao, C. Li, J. Qi, Y. Shi, J. Feng, Combustion joining of carbon-carbon composites to TiAl intermetallics using a Ti-Al-C powder composite interlayer, Compos. Sci. Technol. 115 (2015) 72–79.
[30] J.D.E. White, A.H. Simpson, A.S. Shteinberg, A.S. Mukasyan, Combustion joining of refractory materials: carbon-carbon composites, J. Mater. Res. 23 (2008) 160–169.
[31] K. Uenishi, K.F. Kobayashi, Processing of intermetallic compounds for structural applications at high temperature, Intermetallics 4 (1996) S95–S101.
[32] K. Uenishi, H. Sumi, K.F. Kobayashi, Joining of the intermetallic compound TiAl using self-propagating high-temperature synthesis reaction, Z. Metallkd. 86 (1995) 64–68.
[33] M. Vohra, T.P. Weihs, O.M. Knio, A simplified computational model of the oxidation of Zr/Al multilayers, Combust. Flame 162 (2015) 249–257.
[34] Y.C. Lin, A.A. Nepapushev, P.J. McGinn, A.S. Rogachev, A.S. Mukasyan, Combustion joining of carbon/carbon composites by a reactive mixture of titanium and mechanically activated nickel/aluminum powders, Ceram. Int. 39 (2013) 7499–7505.
[35] B.J. Henz, T. Hawa, M. Zachariah, Molecular dynamics simulation of the energetic reaction between Ni and Al nanoparticles, J. Appl. Phys. 105 (2009) 124310.
[36] A.S. Rogachev, A.S. Mukasyan, Combustion for Material Synthesis, CRC Press, Taylor and Francis, 2015.
[37] Z.A. Munir, U. Anselmi-Tamburini, Self-propagating exothermic reactions: the synthesis of high temperature materials by combustion, Mater. Sci. Rep. 3 (1989) 279–365.
[38] Y. Zu, G. Chen, X. Fu, K. Luo, C. Wang, S. Song, W. Zhou, Effects of liquid phases on densification of TiO_2-doped Al_2O_3-ZrO_2 composite ceramics, Ceram. Int. 40 (2014) 3989–3993.
[39] E. Liu, Y. Bai, Y. Gao, G. Yi, J. Jia, Tribological properties of NiAl-based composites containing Ag_3VO_4 nanoparticles at elevated temperatures, Tribol. Int. 80 (2014) 25–33.
[40] B. Huneau, P. Rogl, K. Zeng, R. Schmid-Fetzer, M. Bohn, J. Bauer, The ternary system Al–Ni–Ti part I: isothermal section at 900 °C; experimental investigation and thermodynamic calculation, Intermetallics 7 (1999) 1337–1345.
[41] J. Liu, J. Cao, X. Lin, H. Chen, J. Wang, J. Feng, Interfacial microstructure and joining properties of TiAl/Ti_3AlC_2 diffusion bonded joints using Zr and Ni foils as interlayer, Vacuum 102 (2014) 16–25.
[42] K. Zhou, Z. Tang, Y. Lu, T. Wang, H. Wang, T. Li, Composition, microstructure, phase constitution and fundamental physicochemical properties of low-melting-point multi-component eutectic alloys, J. Mater. Sci. Technol. 33 (2017) 131–154.
[43] M.L.M. Sistiaga, R. Mertens, B. Vrancken, X. Wang, B.V. Hooreweder, J.-P. Kruth, J.V. Humbeeck, Changing the alloy composition of Al7075 for better processability by selective laser melting, J. Mater. Process. Technol. 238 (2016) 437–445.
[44] A.G. Merzhanov, A.S. Mukasyan, Combustion of Solid Flame, Torus Press, Moscow, 2007.
[45] A. Wolfenden, S.V. Raj, S.K.R. Kondlapudi, Strain-aging and breakaway strain amplitude of damping in NiAl and NiAlZr, J. Mater. Res. 9 (1994) 1166–1173.